

Electronic Supplementary Information (ESI)

Synthesis of triphenylamine-based nanoporous organic polymers for highly efficient captures of SO₂ and CO₂

Jun Yan,*^{a,b} Yan Tan,^{a,c} Sihan Tong,^{a,b} Jiangli Zhu,^{a,b} and Zefeng Wang*^{d,e}

^a*School of Materials Science and Engineering, North Minzu University, Yinchuan 750021, China*

^b*International Scientific and Technological Cooperation Base of Industrial Solid Waste Cyclic Utilization and Advanced Materials, Yinchuan 750021, China*

^c*School of Materials Science and Engineering, Tiangong University, Tianjin 300387, China*

^d*College of Ecology, Lishui University, Lishui 323000, China*

^e*R&D Center of Green Manufacturing New Materials and Technology of Synthetic Leather Sichuan University-Lishui University, Lishui 323000, China*

Corresponding Authors:

Dr. Jun Yan; Email: yanjun2018@nun.edu.cn ;

Dr. Zefeng Wang; Email: shangk72@163.com;

Notes on the SO₂ adsorption test

The sample underwent vacuum degassing at 120°C for 4 hours before conducting the SO₂ adsorption test. For the SO₂ cycle test, the sample was degassed at 120°C under vacuum conditions for 4 hours both before and after the adsorption test. The degassing station is equipped with liquid nitrogen to condense the extracted SO₂ gas, which is then cooled and absorbed by the NaOH alkali solution. The alkali solution is used to absorb the exhaust gas emitted during the test. For the safety of the tester, wearing a 3M gas mask is essential for the tester's safety during the entire test duration. Moreover, the laboratory itself is well-equipped and functions effectively. It is noteworthy that a small leak of SO₂ can generate a strong odor. If your budget permits, it is advisable to select the sulfur dioxide sensor manufactured by Alphasense in the United Kingdom due to safety considerations.

Ideal Adsorbed Solution Theory (IAST) Selectivity

The pure component isotherms of SO₂ and CO₂ were fitted with the dual-site Langmuir-Freundlich (DSLF) model.

$$N = \frac{A_1 \times B_1 \times P^{C_1}}{1 + B_1 \times P^{C_1}} + \frac{A_2 \times B_2 \times P^{C_2}}{1 + B_2 \times P^{C_2}}$$

Where N is molar loading of adsorbate (mmol/g), P is pressure (kPa), A_1 and A_2 are the saturation adsorption capacities (mmol/g) for sites 1 and 2, respectively, B_1 and B_2 are a parameter in the pure component Langmuir isotherm (kPa^{-c1} and kPa^{-c2}), C_1 and C_2 are the parameter of Langmuir-Freundlich for sites 1 and 2, respectively.

Pure-component isotherm fitting parameters were then used for calculating Ideal Adsorbed Solution Theory (IAST)¹ binary-gas adsorption selectivities, S , defined as

$$S = \frac{x_1 / x_2}{y_1 / y_2}$$

$$x_1 + x_2 = 1$$

$$y_1 + y_2 = 1$$

$$\left(\frac{A_1}{C_1} * \ln(1 + B_1(P \frac{y_1}{x_1})^{C1}) + \frac{A_2}{C_2} * \ln(1 + B_2(P \frac{y_1}{x_1})^{C2})\right)_1 = \left(\frac{A_1}{C_1} * \ln(1 + B_1(P \frac{y_2}{x_2})^{C1}) + \frac{A_2}{C_2} * \ln(1 + B_2(P \frac{y_2}{x_2})^{C2})\right)_2$$

In the equation, x_1 and x_2 are the molar fractions of components 1 and 2 in the adsorption phase, and y_1 and y_2 are the molar fractions of components 1 and 2 in the gas phase, respectively. The variable P represents pressure.

Computational details

The first-principles electronic structure investigation of the ANOPs fragment was conducted using the density functional theory (DFT) computational approach. The structure of the ANOPs fragment was optimized using the ω B97XD functional in the Gaussian 03 and GaussView computational packages. Geometry optimization and binding affinities were calculated employing a 6-311++G(d, p) basis set.

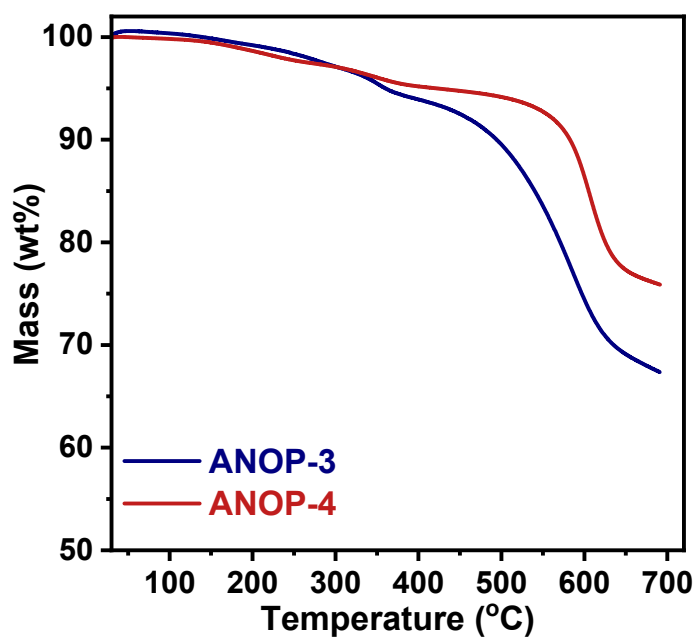


Figure S1. TGA curves of the two ANOPs.

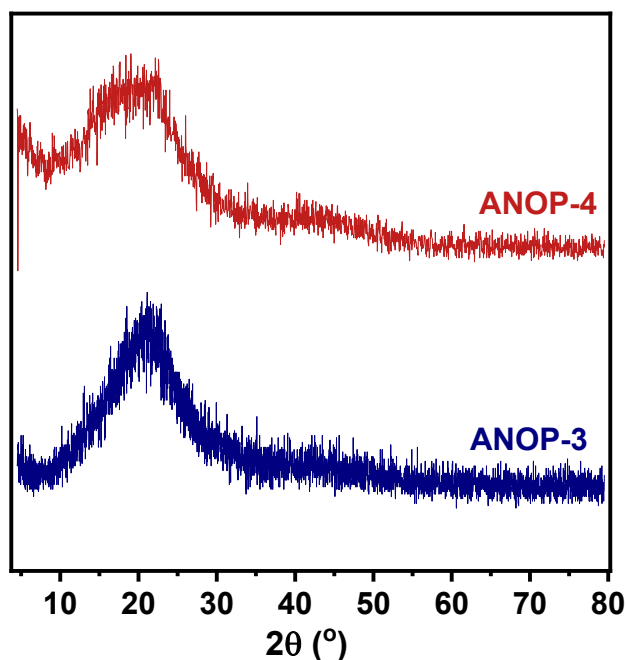


Figure S2. X-ray diffractions of the ANOP-3 and ANOP-4.

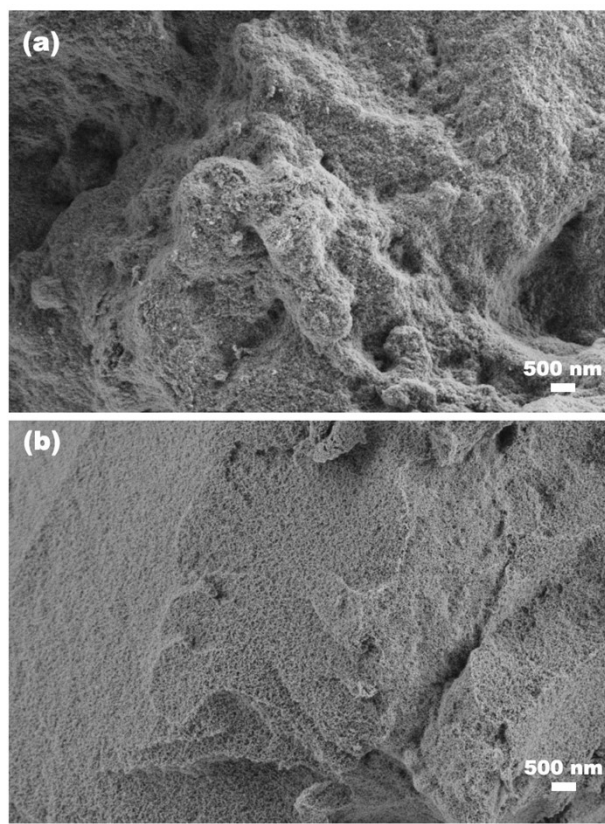


Figure S3. FE-SEM images of ANOP-3 (a) and ANOP-4 (b).

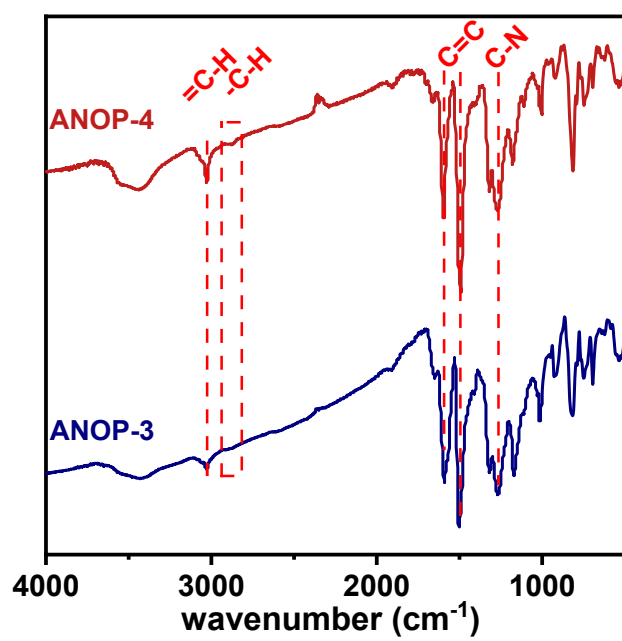


Figure S4. FT-IR spectra of ANOP-3 and ANOP-4.

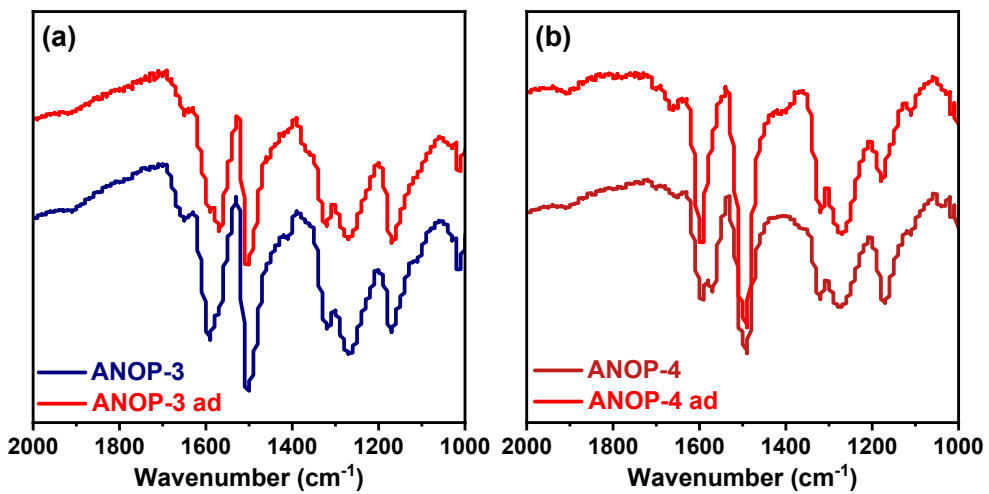


Figure S5. FT-IR spectra of ANOP-3 (a) and ANOP-4 (b) before and after SO₂ adsorption testing.

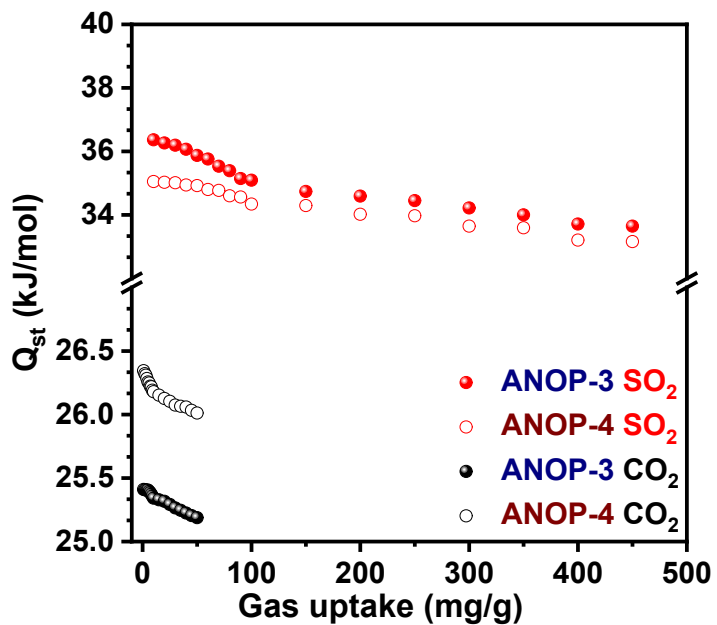


Figure S6. Variation of the adsorption enthalpies for SO₂ and CO₂ with the adsorbed amount in the ANOPs.

Table S1. The chemical composition of ANOPs

Samples	Measured value (wt%)			Theoretical value (wt%)		
	C	H	N	C	H	N
ANOP-3	78.66	4.77	4.86	89.38	5.13	5.49
ANOP-4	84.76	4.86	4.03	90.60	5.17	4.23

Table S2. SO₂ uptake and SO₂/CO₂ selectivity in ANOPs and some reported porous materials

Samples	S _{BET} m ² /g	SO ₂ (mmol/g)		SO ₂ /CO ₂	Ref
		273 K	298 K		
ANOP-3	287	12.5	7.7	64.7	This work
ANOP-4	1016	21.9	10.9	50.5	This work
sPAN-1	113	8.45	5.56	37.6	2
sPAN-2	65	9.36	5.64	50.3	2
HNIP-TBMB-1	45	-	7.20	91	3
HNIP-TBMB-2	155	-	7.07	50	3
HNIP-DCX-1	207	-	4.80	23	3
ELM-12	706	-	2.73	30	4
XJCOF-1	467	11.8	8.4	118	5
XJCOF-2	961	11.1	9.2	39	5
XJCOF-3	503	11.9	9.6	42	5
POP-Py	1074	-	10.8	31	6
POP-BPy	1164	-	12.2	29.8	6
POP-PyI	1087	-	11.0	19.5	6
POP-PyA	536	-	8.1	25.0	6
POP-BPh	965	-	6.5	17.8	6
PDVB	639	-	3.8	19.5	6
TAM-POF	974	13.0	9.45	90	7
ECUTTh-60	472	4.00	3.35	27(1:99)	8
DUT-67	1178	10.3	9.1	37	9
DUT-67-HCl	1349	10.6	9.3	33	9
GU-1	777	8.13	7.60 ^a	15.9 ^a	10
Fe-soc-MOF	1470	-	11.7	32	11
BC-3-650	1449	-	10.7	32	12
BC-4-650	1244	-	9.1	21	12
BC-5-650	1195	-	7.9	22	12
BIDC-2-700	1200	-	10.25	-	13
BIDC-0.5-750	1580	-	15.78	-	13
BIDC-3-800	3750	-	21.42	-	13
NPC-1-800	773.8	-	1.68	-	14
NPC-1-900	1656.2	-	1.85	-	14
NPC-1-1000	1635.2	-	1.39	-	14
NPC-1-1100	1613.5	-	1.26	-	14
NPC-2-800	931.6	-	1.45	-	14
NPC-2-900	1452.3	-	1.60	-	14
NPC-2-1000	1398.3	-	1.35	-	14
NPC-2-1100	1335.2	-	1.22	-	14
GC-2	507	-	10.2	-	15
GC-4	474	-	11.6	-	15

^a296.2

K

Table S3. Dual-site Langmuir-Freundlich simulated parameters for ANOP-3 and ANOP-4.

Samples	Gas	A ₁ (mmol/g)	A ₂ (mmol/g)	B ₁ (kPa ^{-C1})	B ₂ (kPa ^{-C2})	C ₁	C ₂	R ²
ANOP-3	SO₂	12.7719	5.0399	3.6589×10 ⁻⁴	0.1759	1.5003	0.7403	0.9998
	CO₂	0.7455	1.9089	2.6038×10 ⁻²	4.7550×10 ⁻⁴	1.0631	1.4425	0.9999
ANOP-4	SO₂	14.0741	12.3979	7.2017×10 ⁻⁷	6.3007×10 ⁻²	2.6857	0.7890	0.9999
	CO₂	1.6967	1.9219	1.1959×10 ⁻²	3.3473×10 ⁻⁵	1.0280	1.9057	0.9999

Reference

1. A. P. Myers, J. M., *AIChE J.*, 1965, **11**, 7.
2. J. Yan, S. Tong, H. Sun and S. Guo, *J. Mater. Chem. A*, 2023, **11**, 6329-6335.
3. X.-C. An, Z.-M. Li, Y. Zhou, W. Zhu and D.-J. Tao, *Chem. Eng. J.*, 2020, **394**, 124859.
4. Y. Zhang, P. Zhang, W. Yu, J. Zhang, J. Huang, J. Wang, M. Xu, Q. Deng, Z. Zeng and S. Deng, *ACS Appl. Mater. Interfaces*, 2019, **11**, 10680-10688.
5. Y. Fu, Y. Wu, S. Chen, W. Zhang, Y. Zhang, T. Yan, B. Yang and H. Ma, *ACS Nano*, 2021, **15**, 19743-19755.
6. Z. Dai, W. Chen, X. Kan, F. Li, Y. Bao, F. Zhang, Y. Xiong, X. Meng, A. Zheng, F. S. Xiao and F. Liu, *ACS Macro Lett.*, 2022, DOI: 10.1021/acsmacrolett.2c00320, 999-1007.
7. S. Chen, Y. Wu, W. Zhang, S. Wang, T. Yan, S. He, B. Yang and H. Ma, *Chem. Eng. J.*, 2022, **429**.
8. W. Zhang, W. Jia, J. Qin, L. Chen, Y. Ran, R. Krishna, L. Wang and F. Luo, *Inorg. Chem.*, 2022, **61**, 11879-11885.
9. X. H. Xiong, Z. W. Wei, W. Wang, L. L. Meng and C. Y. Su, *J. Am. Chem. Soc.*, 2023, **145**, 14354-14364.
10. J.-Y. Zhang, J.-B. Zhang, M. Li, Z. Wu, S. Dai and K. Huang, *Chem. Eng. J.*, 2020, **391**, 123579.
11. Z. Chen, X. Wang, R. Cao, K. B. Idrees, X. Liu, M. C. Wasson and O. K. Farha, *ACS Materials Lett.*, 2020, **2**, 1129-1134.
12. J. Zhang, P. Zhang, M. Li, Z. Shan, J. Wang, Q. Deng, Z. Zeng and S. Deng, *Ind. Eng. Chem. Res.*, 2019, **58**, 14929-14937.
13. A. J. Richard, Z. Chen, T. Islamoglu, O. K. Farha and H. M. El-Kaderi, *ACS Appl. Mater. Interfaces*, 2022, **14**, 33173-33180.
14. A. Wang, R. Fan, X. Pi, Y. Zhou, G. Chen, W. Chen and Y. Yang, *ACS Appl. Mater. Interfaces*, 2018, **10**, 37407-37416.
15. W.P. Kong, Y. Liu, and J. Liu, *Energy Fuels* 2020, **34**, 3557-3565.